GEOPHYSICAL RESEARCH LETTERS, VOL. 36, L14804, doi:10.1029/2009GL039264, 2009

Enhanced aerosol backscatter adjacent to tropical trade wind clouds revealed by satellite-based lidar

Jason Lucas Tackett[1] and Larry Di Girolamo[1]

Received 19 May 2009; accepted 17 June 2009; published 18 July 2009.

[1] There have been many proposed processes by which clouds modify aerosol properties, suggesting that aerosol properties near clouds are different than far from clouds. We provide the first satellite-based lidar observations of backscatter and color ratio, quantities directly related to aerosol properties, as a function of distance to cloud edge for boundary layer clouds over the western tropical Atlantic. We show backscatter and color ratio are enhanced adjacent to cloud edge, particularly near cloud top and cloud base. Specifically, layer integrated median backscatter increases by 31 ± 3% and 42 ± 2%, at wavelengths of 532 nm, and 1,064 nm, respectively, and layer averaged color ratio increases by 15 ± 5%. Backscatter calculations suggest our observations adjacent to cloud are best explained by an aerosol size distribution with reduced number concentration, increased median radius, and decreased width compared to far from cloud. **Citation:** Tackett, J. L., and L. Di Girolamo (2009), Enhanced aerosol backscatter adjacent to tropical trade wind clouds revealed by satellite-based lidar, *Geophys. Res. Lett.*, *36*, L14804, doi:10.1029/2009GL039264.

1. Introduction

[2] Recent studies have found correlations between cloud and aerosol properties [*Kaufman et al.*, 2005; *Loeb and Schuster*, 2008] along with the potential impact on global radiative forcing [*Chand et al.*, 2009]. These correlations may be caused by passive remote sensing artifacts, aerosol and cloud dependence on large scale meteorology, aerosol influence on cloud properties, or cloud influence on aerosol properties in the near cloud environment due to cloud processing. The first three points have been discussed in detail [*Loeb and Schuster*, 2008], however little has been published concerning the last point, since such observations are difficult to make with confidence. For example, in-situ sampling requires many long aircraft transects to acquire statistically significant results. Passive remote sensors provide large sample sets for estimating aerosol properties, typically aerosol optical depth (AOD), but these estimates can be biased due to 3-D radiative cloud-adjacency effects, whereby solar radiation interacting with the cloud field is scattered by air molecules, aerosols, and the surface into the instruments' field-of-view. This can cause AOD overestimates greater than 100% near cloud edges from passive satellites [*Wen et al.*, 2007; *Yang and Di Girolamo*, 2008], and smaller underestimates from sun-photometers. Active sensing with lidar offers several advantages over passive instruments, including range-resolved backscattered radiances, better cloud detection, and essentially no 3-D radiative cloud-adjacency effects when operated at night. Two notable studies used lidar to observe how aerosol properties change near cloud edge. The first and earliest study qualitatively reported an aerosol backscatter increase near two clouds from a ground-based lidar [*Platt and Gambling*, 1971], while the second study estimated a mean AOD increase of 8∼17% when comparing 4.5 km to 0.1 km from cloud edge using the aircraft-based High Spectral Resolution Lidar (HSRL) [*Su et al.*, 2008]. These studies require further quantitative investigation since measurements were made in daytime (i.e., potential 3-D radiative cloud-adjacency effects) and more samples are necessary for statistical robustness.

[3] Here, we present the first satellite-based lidar observations of aerosol property spatial variability in the vicinity of clouds with the Cloud-Aerosol Lidar with Orthogonal Polarization (CALIOP) instrument. CALIOP provides a larger sample set than previous studies that are unbiased by 3-D radiative cloud-adjacency effects at night. The primary CALIOP products are backscatter at wavelengths of 532 nm and 1,064 nm, denoted by β'_{532} and β'_{1064}, respectively. Backscatter is the fraction of radiance scattered in the backward direction at a given altitude multiplied by the two-way transmittance of the atmosphere above ($km^{-1}sr^{-1}$), and it depends on aerosol composition, size, number concentration, and lidar wavelength. Results are kept in terms of backscatter at the original data resolution (1/3 km horizontal, 30 m vertical), though we provide hypotheses that relate backscatter spatial variability to aerosol property spatial variability. We focus only on single-layer trade wind cumuli over the tropical western Atlantic as part of our ongoing efforts to study clouds, aerosols, and precipitation in conjunction with the Rain In Cumulus over the Ocean (RICO) field campaign [*Rauber et al.*, 2007]. The focus is winter (Dec. – Feb.) to match the RICO time frame.

2. Methodology

[4] We use a combination of CALIOP products to determine backscatter as a function of distance to cloud edge. Cloud locations are provided by the CALIOP Cloud Layer Products (CLP) at three horizontal resolutions: 1/3 km, 1 km, and 5 km. The 1 km and 5 km CLP are created by iterative averaging to reveal optically thin features while the 1/3 km CLP best identifies strongly attenuating boundary layer clouds [*Vaughan et al.*, 2005]. These products were used in two approaches. Approach A used only the 1/3 km resolution CLP, while approach B used both 1/3 km and

[1]Department of Atmospheric Sciences, University of Illinois at Urbana-Champaign, Urbana, Illinois, USA.

0094-8276/09/2009GL039264$05.00

5 km resolution CLP. All clear or cloudy 1/3 km segments that fell within a cloudy 5 km segment were discarded from further analysis in approach B. We examined β'_λ as a function of distance to cloud edges that were detected in the undiscarded 1/3 km resolution CLP in both approaches. Though approach B roughly halved the number of samples meeting our criteria, it did not quantitatively change our conclusions. Thus, we present approach A here. We use the CALIOP Vertical Feature Mask to identify clouds above 8.3 km since the 1/3 km resolution CLP only identifies clouds below this altitude.

[5] Significant averaging is required to reveal aerosol layers in CALIOP backscatter, so we record β'_λ adjacent to cloud edge for many cases and average the ensemble together. Cloud-adjacent profiles can be stored in the CALIOP along-track direction, back-track direction, or both since there are two cloud edges per cloud. Altitude limits of cloud-adjacent profiles are set from cloud top to cloud base for each cloud and only cases meeting the following criteria are used: (1) clouds must be single layered and (2) exist between 0.5 km to 2.0 km in altitude. (3) No clouds must exist above any cloud-adjacent profile since β'_λ is modified by the two-way transmittance of the atmosphere above and (4) the horizontal distance to the next cloud within the altitude limits has to be at least 2.99 km. All profiles satisfying these criteria are stored at increasing distance from cloud edge until either one-half the horizontal distance to the next cloud or 2.99 km, which ever is shorter. They are stored in this manner since we are often simultaneously moving away from one cloud and approaching another. Thus, we observe backscatter as a function of distance from the nearest cloud edge rather than distance to the next cloud edge. The horizontal distance 2.99 km was selected since β'_λ did not change appreciably at further distances from cloud edge. For nighttime orbits in Dec. 2006 – Feb. 2007, Dec. 2007 – Feb. 2008, and Dec. 2008 – Feb. 2009, there are 26,833 clouds and 34,371 cloud edges satisfying these criteria in our tropical western Atlantic domain (5°N–25°N, 45°W–75°W). The total number of β'_λ samples as a function of altitude and distance to cloud edge is plotted in Figure S1 of the auxiliary material.[1] Most samples occur within the altitude range 0.6 km to 1.0 km. A power law fit to the sampled cloud chord lengths gives a dimension of 2.45, with 85% having lengths $\leq$ 1 km. Our observed cloud altitude and size distribution are consistent with previous observations of trade wind cumuli in this region [*Zhao and Di Girolamo*, 2007].

3. Results

[6] Figure 1a shows median β'_{532} adjacent to all cloud edges meeting the criteria in our Methodology section. There are two clear trends. First, median β'_{532} increases towards lower altitudes since more aerosols exist near the surface. Second, median β'_{532} increases as cloud edge is approached at all altitudes. The same trends are evident in median β'_{1064} (Figure S2). Backscatter enhancement adjacent to cloud edge is best demonstrated by dividing median β'_{532} at each altitude by the horizontal average of all median β'_{532} occurring within 2.99 km of cloud edge at that altitude. These normalized median β'_{532}, shown in Figure 1b, provide a unique observation: maximum backscatter enhancement occurs adjacent to tops of thick clouds (tops $\sim$ 2 km) and near cloud base. There are several processes that may give rise to these enhancements. Evaporated cloud droplets create regions of enhanced humidity [*Perry and Hobbs*, 1996; *Laird*, 2005], causing aerosols to become larger due to hygroscopic growth; this enhances backscatter [*Su et al.*, 2008]. Regions of enhanced humidity have the greatest horizontal extent near cloud top when an overlying stable layer exists [*Perry and Hobbs*, 1996; *Lu et al.*, 2003], which in the tropics occurs around an altitude of 2 km [*Rauber et al.*, 2007]. Also at cloud top, detrained cloud drops evaporate and leave behind larger, but fewer, aerosols compared to the entrained air due to droplet collision-coalescence within the cloud [*Roelofs and Kamphuis*, 2009]. Collision-coalescence occurs more often in thicker clouds, so its impact on aerosol size and hence, backscatter, is greatest at the tops of thicker clouds. Meanwhile, lateral mixing with dry air adjacent to cloud causes descending motion due to evaporative cooling [*Heus et al.*, 2008], which may transport larger aerosols near cloud top to mid-cloud levels, enhancing backscatter. The backscatter enhancement maximum at lower altitudes (0.5 km to 0.75 km) is adjacent to cloud bases, most of which are from small and shallow cumuli [*Zhao and Di Girolamo*, 2007], and is possibly due to vertical advection of humid air below cloud base [*Perry and Hobbs*, 1996] causing aerosol hygroscopic growth. Median color ratio $\chi' = \beta'_{1064}/\beta'_{532}$ in Figure 1c also exhibits enhancement near cloud edge with maxima at similar altitudes as β'_{532} maxima. Color ratio depends strongly on particle size, bolstering the hypothesis that aerosols are largest near the top of thick clouds and cloud base.

[7] Horizontal backscatter variability is illustrated by vertically integrating median β'_{532} and median β'_{1064} in Figures 1a and S2, respectively, from 0.5 km to 2.0 km. Integrated median backscatter is denoted by γ'_λ (sr^{-1}). The result in Figure 2 unequivocally shows γ'_λ is enhanced adjacent to cloud edge. Specifically, as summarized in Table 1, γ'_{532} and γ'_{1064} increase by 31 ± 3% and 42 ± 2%, respectively, when comparing 2.99 km to 0.33 km from cloud edge. The aircraft study using HSRL found a 26–30% increase in β'_{532} when comparing 4.5 km to 0.1 km from cloud edge at particular reference altitudes [*Su et al.*, 2008]. Our results are consistent since $\beta'_{532} \propto \gamma'_{532}$, bearing in mind that we focus on a large sample of clouds at night while they focus on a smaller sample of clouds in the day. We also vertically average the median χ' in Figure 1c from 0.5 km to 2.0 km and plot the result in Figure S3. We find $\Delta\chi' = 15 \pm 5\%$ when comparing 2.99 km to 0.33 km from cloud edge.

[8] The observed backscatter and color ratio increases adjacent to cloud edge may result from changes in the aerosol size distribution by several processes. Hygroscopic growth increases both the median radius R and width σ, leaving number concentration N unchanged [*Gerber*, 1985]. Droplet collision-coalescence decreases N and increases R, though precipitation scavenging efficiently removes the largest cloud droplets, thereby decreasing σ [*Peter et al.*, 2006; *Roelofs and Kamphuis*, 2009] and limiting the in-

[1] Auxiliary materials are available in the HTML. doi:10.1029/2009GL039264.

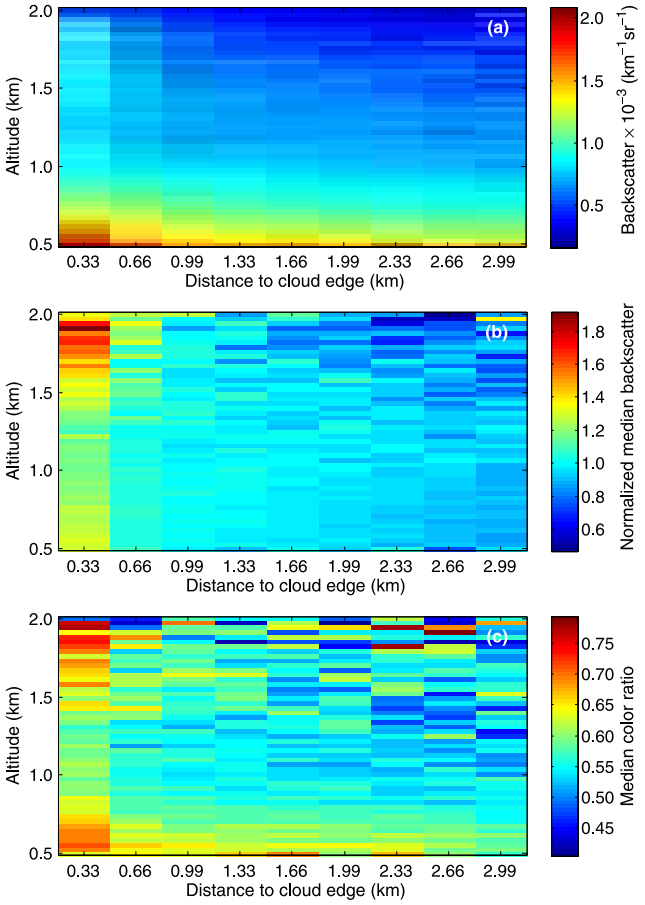

Figure 1. (a) Median backscatter at 532 nm. (b) Median backscatter at 532 nm normalized at each altitude by the horizontal average of median backscatter within 2.99 km of cloud edge at that altitude. Values greater than one indicate median backscatter is above the average median backscatter at that altitude. (c) Median color ratio.

crease in R. Other scavenging processes (nucleation, diffusion, and impaction scavenging) decrease N and increase σ [*Flossmann et al.*, 1985]. We perform backscatter calculations to understand what changes in a typical maritime aerosol size distribution would produce our observations in Table 1. We assume aerosol composition is ammonium sulfate for $r \leq 0.2$ μm, and sea salt for $r > 0.2$ μm, typical for this region [*Peter et al.*, 2008]. Refractive indices for ammonium sulfate and sea salt are from Andrew Lacis' Database of Aerosol Refractive Indices (http://gacp.giss.nasa.gov/data_sets/) and the Optical Properties of Aerosols and Clouds (OPAC) software [*Hess et al.*, 1998], respectively. The assumed aerosol size distribution far from cloud is the OPAC "Maritime clean" tri-modal lognormal distribution at ambient RH = 80% where each mode j is defined by a median radius R_j, total number concentration N_j, and width σ_j. We assume N_j exponentially decreases in the vertical with a one kilometer scale height and we perform Mie calculations for the scattering cross section and scattering phase function. To determine the change in γ'_λ due to a change in the size distribution, all modes of a parameter R_j, N_j, or σ_j are increased by the same amount, holding the other two parameters fixed. The percent change $\Delta\gamma'_\lambda$ is the fractional increase of the modified γ'_λ versus the original γ'_λ far from cloud, times 100%. Percent change in color ratio $\Delta\chi'$ is computed similarly. Changing the parameter modes separately for each parameter may yield different results, but doing so requires interpreting more degrees of freedom than are available, i.e., our three observations.

[9] The results of our calculations in Table 1 suggest a ~13% increase in R_j alone can explain $\Delta\gamma'_\lambda$ at both wavelengths, but not $\Delta\chi'$, which would require a 26% increase in R_j alone. This suggests hygroscopic growth is not the only process affecting aerosol properties. A 34% N_j increase alone accounts for $\Delta\gamma'_\lambda$, but not $\Delta\chi'$ since χ' depends weakly on N_j. Thus, an increase in N_j alone cannot account for all our observations. A ~6% increase in σ_j alone can roughly explain both $\Delta\gamma'_\lambda$ and $\Delta\chi'$, suggesting collision-coalescence and/or other scavenging processes may have broadened the size distribution width. However, these processes do not act on σ_j alone, but also on N_j. Hence, all three aerosol size distribution parameters likely change as cloud edge is approached. We use a chi-squared minimization method to estimate the combination of ΔR_j, ΔN_j, and $\Delta\sigma_j$ that best fits our three observations in Table 1 by minimizing equation (1). Here, the subscript *obs* refers to observed changes while $\Delta\gamma'_\lambda$ and $\Delta\chi'$ are calculated with different permutations of ΔR_j, ΔN_j, and $\Delta\sigma_j$.

$$chi-squared = \frac{\left(\Delta\gamma'_{532,obs} - \Delta\gamma'_{532}\right)^2}{\Delta\gamma'_{532,obs}} + \frac{\left(\Delta\gamma'_{1064,obs} - \Delta\gamma'_{1064}\right)^2}{\Delta\gamma'_{1064,obs}} + \frac{\left(\Delta\chi'_{obs} - \Delta\chi'\right)^2}{\Delta\chi'_{obs}} \quad (1)$$

We find that a 34% increase in R_j, 32% decrease in N_j, and a 2% decrease in σ_j provide the best fit (yielding $\Delta\gamma'_{532}$ = 28%, $\Delta\gamma'_{1064}$ = 45%, and $\Delta\chi'$ = 14%). This particular combination of changes results in a 16% AOD increase near cloud edge at 532 nm wavelength. Sun-photometer measurements from two recent studies yield comparable AOD increase estimates near cloud edge of ~10% [*Redemann et al.*, 2009] and ~13% [*Koren et al.*, 2007] at visible wavelengths, bearing in mind that our analysis is at night, while theirs is during the day which may cause AOD underestimates due to 3-D radiative cloud-adjacency effects. A simultaneous increase in R_j and decrease in N_j and

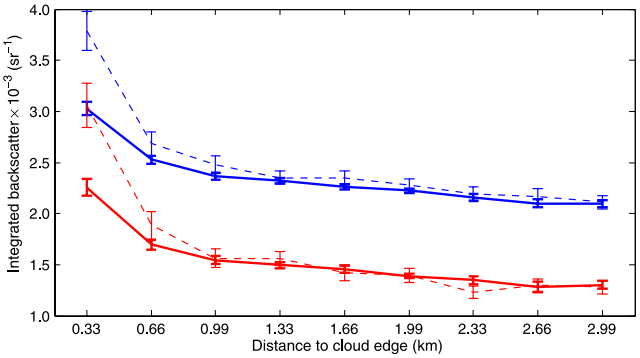

Figure 2. Vertically integrated median backscatter at 532 nm (blue) and 1,064 nm (red) for night (solid lines) and day (dashed lines). Error bars are the propagated standard error on the median backscatter [*Yule*, 1911].

Table 1. Observed Increases in Nighttime Integrated Median Backscatter and Vertically Averaged Median Color Ratio When Comparing 2.99 km to 0.33 km From Cloud Edge With Changes in Assumed Aerosol Size Distribution Parameters and Cloud Droplet Number Concentration Required to Explain Them[a]

	Observed Increase (%)	ΔR_j (%)	$\Delta\sigma_j$ (%)	ΔN_j (%)	Cloud Droplets Added (cm^{-3})
$\Delta\gamma'_{532}$	31 ± 3	12 ± 1	7.5 ± 0.5	34 ± 3	0.018 ± 0.002
$\Delta\gamma'_{1064}$	42 ± 2	13 ± 1	6 ± 0.5	34 ± 3	0.011 ± 0.001
$\Delta\chi'$	15 ± 5	26 ± 8	5 ± 2	>100	0.007 ± 0.003
Chi-squared best fit		34	−2	−32	

[a]Errors bars are the propagated standard error on the median [*Yule*, 1911]. The final row shows the parameter change combination that best fits our observations using a chi-squared minimization method.

σ_j is consistent with collision-coalescence with larger aerosols removed by precipitation scavenging, although precipitation scavenging may be minimal given that only ~5% of these clouds precipitate [*Snodgrass et al.*, 2009]. The increase in R_j also suggests hygroscopic growth. We note that a 34% increase in R_j is consistent with an RH increase from 80% to 94% [*Hess et al.*, 1998], a reasonable RH increase near marine clouds [*Twohy et al.*, 2009]. However, hygroscopic growth and scavenging processes broaden the distribution width, which is not deduced by the best fit. That no single process explains all our observations suggests several of these concurrent processes may be equally important in controlling the aerosol size distribution adjacent to cloud.

4. Potential Cloud Artifacts

[10] We must address the possibility of cloud droplets existing in the first "clear air" sample near cloud edge which would also enhance backscatter. Adding a gamma cloud droplet size distribution with a 10 μm effective radius to the "Maritime clean" aerosol size distribution reveals a cloud droplet number concentration < 0.02 cm^{-3} could explain $\Delta\gamma'_\lambda$ or $\Delta\chi'$. However, different concentrations are required for $\Delta\gamma'_{532}$, $\Delta\gamma'_{1064}$, and $\Delta\chi'$, which suggests cloud contamination is not the only explanation – aerosol properties must change as well. The impact of cloud contamination is also reduced in our analysis by choosing median γ'_λ, since the mean is strongly influenced by extreme backscatter values likely due to cloud droplets. The quartiles of the γ'_λ distribution plotted in Figure S4 show enhanced backscatter near cloud edge even for the lowest quartile.

[11] As backscatter is stored at increasing distance from cloud edge, clouds outside of the lidar transect may modify aerosol properties within these profiles. To determine the influence of these off-transect clouds on average backscatter, we simulated 2-D fields of circular clouds with backscatter decaying exponentially from cloud edge [*Tackett*, 2009]. Averaging random transects through the cloud field revealed the exponentially decaying functionality was preserved within the e-folding distance to cloud edge, then approached a constant backscatter offset at further distances as observed in Figure 2.

[12] We avoid 3-D radiative cloud-adjacency effects from artificially enhancing backscatter near cloud edge by focusing on nighttime. However, daytime scenes were examined. Figure 2 shows daytime median γ'_λ (dashed lines) exhibits a steeper gradient near cloud edge compared to nighttime. This is consistent with 3-D radiative cloud-adjacency effects, although diurnal variations in aerosol properties, boundary layer depth, or photochemical aerosol production [*Perry and Hobbs*, 1994] are also plausible explanations.

5. Conclusion

[13] Our observations of backscatter enhancement adjacent to cloud edge demonstrate that clouds influence aerosol properties in their vicinity. The magnitude of enhancement is greatest near cloud top and cloud base, which may be in part due to (1) detrainment of enlarged aerosols through collision-coalescence and (2) stable layer capping of enhanced moisture and vertical moisture advection causing hygroscopic growth. We observed increases in layer integrated backscatter at 532 nm and 1,064 nm and layer average color ratio of 31 ± 3%, 42 ± 2% and 15 ± 5%, respectively, when comparing 2.99 km to 0.33 km from cloud edge. Our backscatter calculations suggest that multiple cloud processing mechanisms act in concert to modify the aerosol size distribution and produce these enhancements, making it difficult to decouple the relative influence of each. Fortunately, these unique observations now provide valuable validation data for cloud-resolving models that include dynamic and chemical aerosol processing, since backscatter is easily calculated given the modeled aerosol size distribution. Validated models can deduce the relative influence of each cloud processing mechanisms on aerosol populations to identify the most important processes to include in climate models.

[14] Though we chose winter to coincide with the RICO campaign timeframe, we find the enhancement of γ'_λ is consistent for the remaining three seasons. However, the overall magnitude of γ'_λ varies by 40% between seasons, which may be explained by seasonal variability of dust and smoke advected from Africa over the tropical western Atlantic [*Prospero and Lamb*, 2003]. The mechanisms causing diurnal and seasonal variability in backscatter enhancement adjacent to cloud edge remain the topic of future research.

[15] **Acknowledgments.** This research was supported by the National Science Foundation (NSF) under grant ATM-03-46172. CALIOP data were obtained from the NASA Langley Research Center Atmospheric Science Data Center. The authors thank Professor Robert Rauber and the UIUC RICO group for valuable discussions.

References

Chand, D., R. Wood, T. L. Anderson, S. K. Satheesh, and R. J. Charlson (2009), Satellite-derived direct radiative effect of aerosols dependent on cloud cover, *Nat. Geosci.*, *2*, 181–184, doi:10.1038/ngeo437.

Flossmann, A. I., W. D. Hall, and H. R. Pruppacher (1985), A theoretical study of the wet removal of atmospheric pollutants. Part I: The redistribution of aerosol particles captured through nucleation and impaction scavenging by growing cloud drops, *J. Atmos. Sci.*, *42*, 583–606, doi:10.1175/1520-0469(1985)042<0583:ATSOTW>2.0.CO;2.

Gerber, H. E. (1985), Relative humidity parameterization of the Navy Aerosol Model (NAM), *NRL Rep. 8956*, Naval Res. Lab., Washington, D. C.

Hess, M., P. Koepke, and I. Schult (1998), Optical properties of aerosols and clouds: The software package OPAC, *Bull. Am. Meteorol. Soc.*, *79*, 831–844, doi:10.1175/1520-0477(1998)079<0831:OPOAAC>2.0.CO;2.

Heus, T., G. van Dijk, H. J. J. Jonker, and H. E. A. Van den Akker (2008), Mixing in shallow cumulus clouds studied by Lagrangian particle tracking, *J. Atmos. Sci.*, *65*, 2581–2597, doi:10.1175/2008JAS2572.1.

Kaufman, Y. J., I. Koren, L. A. Remer, D. Rosenfeld, and Y. Rudich (2005), The effect of smoke, dust, and pollution aerosol on shallow cloud development over the Atlantic Ocean, *Proc. Natl. Acad. Sci. U. S. A.*, *102*, 11,207–11,212, doi:10.1073/pnas.0505191102.

Koren, I., L. A. Remer, Y. J. Kaufman, Y. Rudich, and J. V. Martins (2007), On the twilight zone between clouds and aerosols, *Geophys. Res. Lett.*, *34*, L08805, doi:10.1029/2007GL029253.

Laird, N. F. (2005), Humidity halos surrounding small cumulus clouds in a tropical environment, *J. Atmos. Sci.*, *62*, 3420–3425, doi:10.1175/JAS3538.1.

Loeb, N. G., and G. L. Schuster (2008), An observational study of the relationship between cloud, aerosol and meteorology in broken low-level cloud conditions, *J. Geophys. Res.*, *113*, D14214, doi:10.1029/2007JD009763.

Lu, M.-L., J. Wang, A. Freedman, H. H. Jonsson, R. C. Flagan, R. A. McClatchey, and J. H. Seinfeld (2003), Analysis of humidity halos around trade wind cumulus clouds, *J. Atmos. Sci.*, *60*, 1041–1059, doi:10.1175/1520-0469(2003)60<1041:AOHHAT>2.0.CO;2.

Perry, K. D., and P. V. Hobbs (1994), Further evidence for particle nucleation in clear air adjacent to marine cumulus clouds, *J. Geophys. Res.*, *99*, 22,803–22,818, doi:10.1029/94JD01926.

Perry, K. D., and P. V. Hobbs (1996), Influences of isolated cumulus clouds on the humidity of their surroundings, *J. Atmos. Sci.*, *53*, 159–174, doi:10.1175/1520-0469(1996)053<0159:IOICCO>2.0.CO;2.

Peter, J. R., S. T. Siems, J. B. Jensen, J. L. Gras, and J. M. Hacker (2006), Prediction and observation of cloud processing of the aerosol size distribution by a band of cumulus, *Q. J. R. Meteorol. Soc.*, *132*, 845–863, doi:10.1256/qj.05.106.

Peter, J. R., A. M. Blyth, B. Brooks, J. B. McQuaid, J. J. N. Lingard, and M. H. Smith (2008), On the composition of Caribbean maritime aerosol properties measured during RICO, *Q. J. R. Meteorol. Soc.*, *134*, 1059–1063, doi:10.1002/qj.198.

Platt, C. M. R., and D. J. Gambling (1971), Laser radar reflexions and downward infrared flux enhancement near small cumulus clouds, *Nature*, *232*, 182–185, doi:10.1038/232182a0.

Prospero, J. M., and P. J. Lamb (2003), African droughts and dust transport to the Caribbean: Climate change implications, *Science*, *302*, 1024–1027, doi:10.1126/science.1089915.

Rauber, R. M., et al. (2007), Rain in shallow cumulus over the ocean: The RICO campaign, *Bull. Am. Meteorol. Soc.*, *88*, 1912–1928, doi:10.1175/BAMS-88-12-1912.

Redemann, J., Q. Zhang, P. B. Russell, J. M. Livingston, and L. A. Remer (2009), Case studies of aerosol remote sensing in the vicinity of clouds, *J. Geophys. Res.*, *114*, D06209, doi:10.1029/2008JD010774.

Roelofs, G. J., and V. Kamphuis (2009), Cloud processing, cloud evaporation and Angström exponent, *Atmos. Chem. Phys.*, *9*, 71–80.

Snodgrass, E. R., L. Di Girolamo, and R. M. Rauber (2009), Precipitation characteristics of trade wind clouds during RICO derived from radar, satellite, and aircraft measurements, *J. Appl. Meteorol. Climatol.*, *48*, 464–483, doi:10.1175/2008JAMC1946.1.

Su, W., G. L. Schuster, N. G. Loeb, R. R. Rogers, R. A. Ferrare, C. A. Hostetler, J. W. Hair, and M. D. Obland (2008), Aerosol and cloud interaction observed from high spectral resolution lidar data, *J. Geophys. Res.*, *113*, D24202, doi:10.1029/2008JD010588.

Tackett, J. L. (2009), Aerosol spatial variability in the vicinity of marine boundary layer clouds observed by satellite-based lidar, M.S. thesis, Dep. of Atmos. Sci., Univ. of Ill. at Urbana-Champaign, Urbana.

Twohy, C. H., J. A. Coakley Jr., and W. R. Tahnk (2009), Effect of changes in relative humidity on aerosol scattering near clouds, *J. Geophys. Res.*, *114*, D05205, doi:10.1029/2008JD010991.

Vaughan, M. A., D. M. Winker, and K. A. Powell (2005), CALIOP algorithm theoretical basis document—Part 2: Feature detection and layer properties algorithms, *Rep. PC-SCI-202*, NASA Langley Res. Cent., Hampton, Va.

Wen, G., A. Marshak, R. F. Cahalan, L. A. Remer, and R. G. Kleidman (2007), 3-D aerosol-cloud radiative interaction observed in collocated MODIS and ASTER images of cumulus cloud fields, *J. Geophys. Res.*, *112*, D13204, doi:10.1029/2006JD008267.

Yang, Y., and L. Di Girolamo (2008), Impacts of 3-D radiative effects on satellite cloud detection and their consequences on cloud fraction and aerosol optical depth retrievals, *J. Geophys. Res.*, *113*, D00B07, doi:10.1029/2008JD009945.

Yule, G. U. (1911), *An Introduction to the Theory of Statistics*, 376 pp., C. Griffin, London.

Zhao, G., and L. Di Girolamo (2007), Statistics on the macrophysical properties of trade wind cumuli over the tropical western Atlantic, *J. Geophys. Res.*, *112*, D22S03, doi:10.1029/2006JD007384.

L. Di Girolamo and J. L. Tackett, Department of Atmospheric Sciences, University of Illinois at Urbana-Champaign, 105 South Gregory Street, Urbana, IL 61801-3070, USA. (tackett2@atmos.uiuc.edu)